

MACHINE LEARNING-DRIVEN COMPUTATIONS OF 3D COHERENT SYNCHROTRON RADIATION *

C. Leon [†], P. M. Anisimov, N. Yampolsky, A. Scheinker
Los Alamos National Laboratory, Los Alamos, NM, USA

Abstract

As electrons are accelerated, for instance, along curved paths in a magnetic field within a particle accelerator, they emit synchrotron radiation. When the wavelength of this radiation exceeds the bunch length, it becomes coherent, leading to significant alterations in the phase space distribution of the electrons. Simulating the effects of coherent synchrotron radiation is a highly resource-intensive task in accelerator physics. In this work, we demonstrate the application of a modified U-Net model to generate 3D wakefields from electron distributions. Our results demonstrate that the machine learning model can generate accurate wakefields much faster than traditional methods, while also effectively generalizing beyond its training dataset.

INTRODUCTION

Coherent Synchrotron Radiation (CSR) can substantially modify the electron distribution in circular orbits, as observed in systems like electron storage rings or bunch compressors. When the emitted wavelength, λ , is much larger than the bunch size, the bunch appears as a point source at λ -resolution, with all N_e electrons exhibiting nearly identical motion. As a result, the emitted radiation from these electrons is roughly in phase, leading to coherent addition of the radiation and an intensity scaling as $\mathcal{O}(N_e^2)$. This coherence effect can significantly alter the phase space distribution of the bunch. In the ultra-relativistic regime, this primarily manifests as energy loss in the tail and center of the bunch, while the head gains energy, contributing to an increase in the overall emittance.

The force experienced by an electron due to radiation emitted by other electrons in the past is termed the wakefield, $W(r, t)$. To calculate this wakefield, one must integrate the Lorentz force, $F(r, t)$, derived from the Liénard-Wiechert fields, over the past light cone:

$$W(r) = \int_{\Delta} d^3 r' \lambda(r', t') F(r', t') \Big|_{ret.} . \quad (1)$$

Here, Δ denotes the past light cone, the time variable in the integrand corresponds to the retarded time, and $\lambda(r', t')$ represents the particle density. The computational burden of handling retarded time evaluations, along with the $\mathcal{O}(N_e^2)$ interactions (where N_e typically reaches 10^{10}), makes performing CSR calculations extremely resource-intensive. This challenge has led to the use of approximations, such as the 1D model [1]. However, even under the 1D approximation,

* Work was supported by the Los Alamos National Laboratory Laboratory Directed Research and Development (LDRD) DR project 20220074DR.
† cleon@lanl.gov

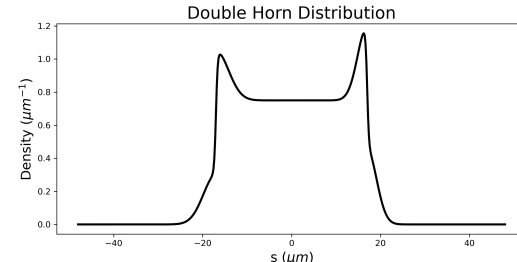


Figure 1: Double-Horn 1D Profile.

incorporating CSR into simulations can increase processing time by a factor of ten [2]. As a result, traditional simulation methods often become too slow for certain use cases, particularly when optimizing accelerator designs through comprehensive parameter space exploration. Given the trend toward smaller bunch sizes in modern accelerators, the need for fast and precise 3D CSR modeling has become increasingly important, as this becomes important in constraints, shown in Table 1.

Machine learning (ML) can speed up simulations to provide real-time virtual diagnostics which can be used for real-time adaptive beam control. For example, in [3] the first approach to adaptive ML was demonstrated combining a deep learning with adaptive feedback [4] for automatic control of the longitudinal phase space of the LCLS FEL electron beam. They can also be used to speed up accelerator simulations [5, 6]. Convolutional neural network (CNN) computations utilize matrix multiplications and several parallelized operations and with modern GPU's, which are optimized for such tasks, can be performed rapidly. Hence, a CNN trained on CSR simulations data can lead to very fast computations.

Here, we take previous a CNN model trained to predict the fully 3D wakefields generated by electrons at steady-state [7] and see its generalization ability. Specifically, we investigate at how well it performs on multi-Gaussian in the test set. In addition, we test how well it performs on out of distribution

Table 1: Characteristics of Dataset

Multi-Gaussian Dataset	
Physical Range	$x_i \in (-48, 48) \mu\text{m}$ $i = s, x, y$
Distribution	Sum of 2 to 25 Gaussians
Attributes	$\mu_i \in (-12, 12) \mu\text{m}$ $\sigma_i \in (2, 12) \mu\text{m}$

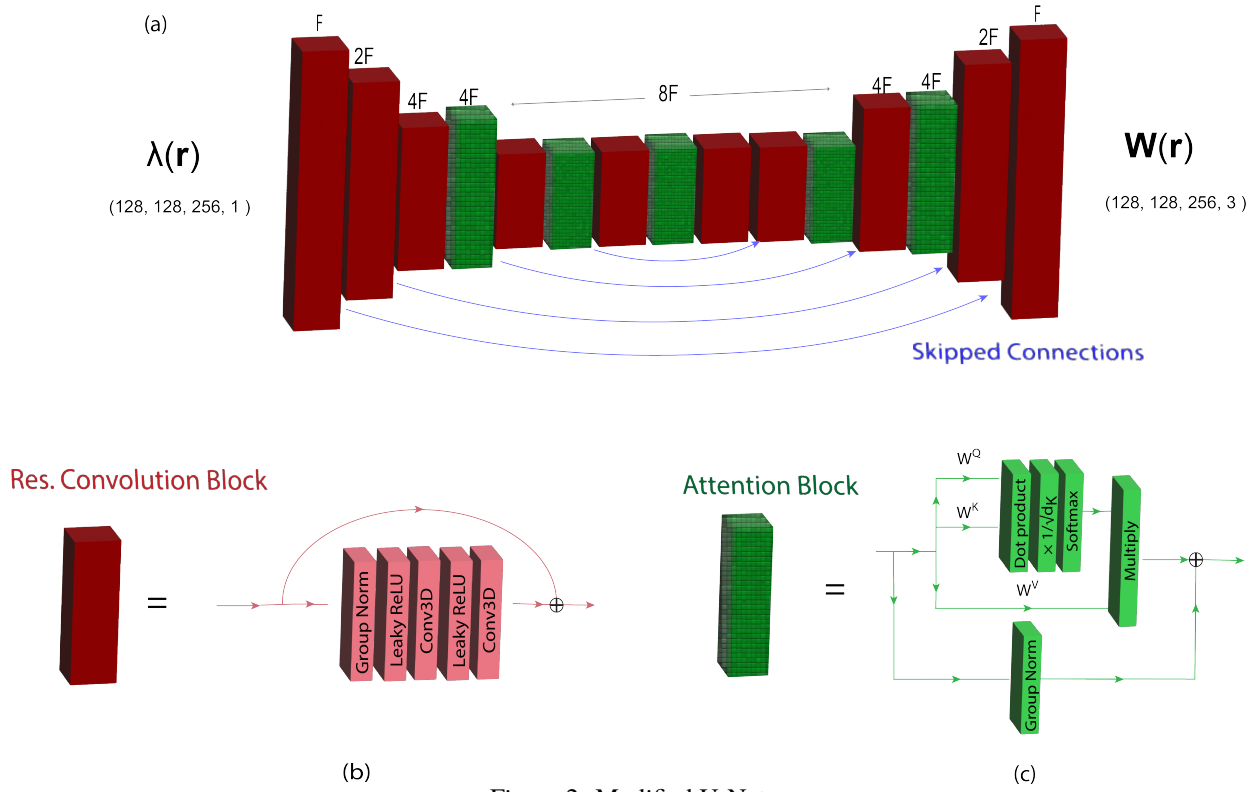


Figure 2: Modified U-Net.

(OOD) generalization, using a Double Horn distribution, of which the model has never encountered before.

DATA

The data used here comes from the conventional (i.e., non-ML) software PyCSR3D [2, 8], whose physics formulation is based on the Hamiltonian approach in Synder-Courant theory developed by Cai and Ding. [9–11]. It is assumed the bunch is in a steady state condition (i.e., not transient) and that the shielding suppression of lower frequencies from the metallic cavity is negligible.

The Frenet-Serret coordinates with the reference path of circular motion in the horizontal plane is used. Here, the longitudinal component s is the arc length, the horizontal x is the radial outward distance from the circle, while y is the vertical distance from the horizontal plane. Details of the dataset can be seen in Table 1. 500 simulations were produced, 425 were used for training and 75 for test.

A double horn distribution was put into PyCSR3D to obtain its generated wakefield. The 1D profile of the distribution in the longitudinal direction can be seen Fig. 1. For the transverse dependence, we used a Gaussian.

MODEL

The model considered here will be labeled λ -NN, which sends the density to wakefield:

$$\lambda\text{-NN} : \lambda(\mathbf{r}) \rightarrow \mathbf{W}(\mathbf{r}). \quad (2)$$

In terms of arrays, $(128, 128, 256, 1) \rightarrow (128, 128, 256, 3)$. This followed a modified U-Net architecture [12], which can be seen in Fig. 2.

We first pre-trained λ -NN on a Gaussian Dataset and trained on the Multi-Gaussian Dataset.

RESULTS

To evaluate the models, we used the relative weighted mean average error (RW-MAE) for each component $i = s, x, y$:

$$\text{RW-MAE}_i = \frac{\int d^3\mathbf{r} \lambda(\mathbf{r}) |W_{\text{pred.}}^i(\mathbf{r}) - W_{\text{true}}^i(\mathbf{r})|}{\int d^3\mathbf{r} \lambda(\mathbf{r}) |W_{\text{true}}^i(\mathbf{r})|}, \quad (3)$$

where $W_{\text{true}}^i(\mathbf{r})/W_{\text{pred.}}^i(\mathbf{r})$ is the true/predicted values for the wakefield. The idea behind this is that we care most about being correct where there are more particles, since $\mathbf{W}(\mathbf{r})$ is being used to update the phase space. Moreover, this metric differs quite a bit from the mean squared error loss (MSE) used in training, thus providing a complementary measure to the optimized MSE.

An example of predictions versus truth in the test can be seen in Fig. 3. The results of the trained network on the training and test set can be seen in Table 2. Specifically, comparing the results in Table 2 shows that the performance of the model on train and test set is relatively comparable.

For the Double Horn distribution, we find that the RW-MAE were 16.8%, 3.1%, and 5.6% for W_s , W_x and W_y , respectively. This is somewhat higher than on Multi-Gaussian errors, which is not surprising since this is a OOD prediction.

Table 2: Results of U-Net on Training and Test Data

Model	Set	s Mean (STD), %	x Mean (STD), %	y Mean (STD), %
λ -NN-Multi	Training	3.60 (1.51)	0.96 (0.41)	2.56 (0.76)
	Test	3.60 (1.51)	0.99 (0.56)	2.74 (0.92)

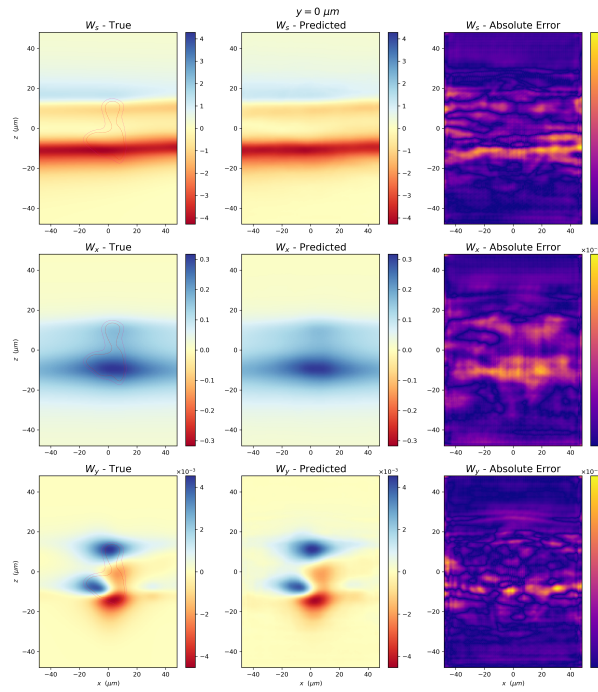


Figure 3: An example of the predicted wakefield for a Multi-Gaussian distribution in the test set.

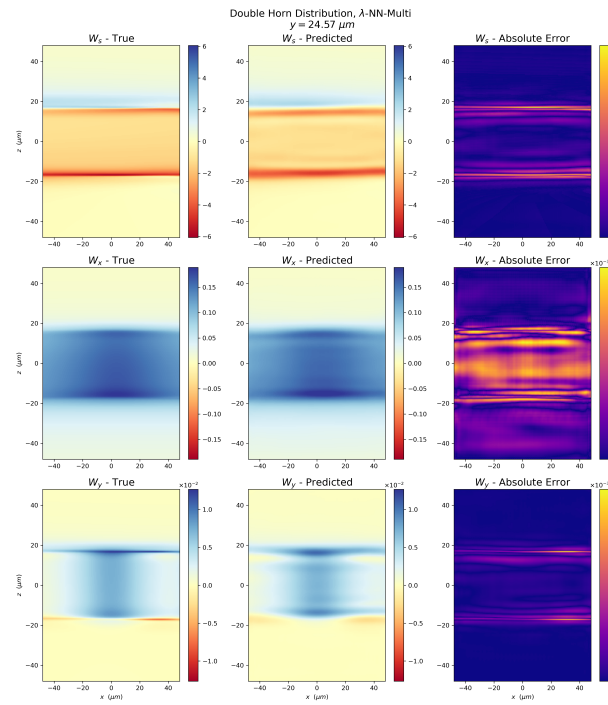


Figure 4: 2D Projections of the predicted wakefield for a Double Horn distribution.

A cross section of the predicted wakefield patterns can be seen in Fig. 4; it is evident that these patterns happen to qualitatively capture the wakefield reasonably well.

CONCLUSION

We have developed a surrogate ML model that can accurately predict 3D wakefields of electrons in the steady state condition. We investigated the generalization ability of the models, specifically on the Multi-Gaussian test dataset and a Double Horn distribution.

Future work could integrate physical principles directly into the neural networks, as prior studies have demonstrated that this approach enhances prediction accuracy and generalization capabilities [13, 14]. Expanding the diversity of distributions within the training dataset would further strengthen the robustness of the λ -NN model. Additionally, while the beam energy was held constant in this work, future studies could incorporate it as a dynamic input to the networks for more comprehensive modeling.

REFERENCES

- [1] M. Borland, “Simple method for particle tracking with coherent synchrotron radiation”, *Phys. Rev. ST Accel. Beams*, vol. 4, no. 7, p. 070 701, 2001.
doi:10.1103/PhysRevSTAB.4.070701
- [2] C. Mayes, “Computational approaches to coherent synchrotron radiation in two and three dimensions”, *J. Instrum.*, vol. 16, no. 10, p. P10010, 2021.
doi:10.1088/1748-0221/16/10/P10010
- [3] A. Scheinker, A. Edelen, D. Bohler, C. Emma, and A. Lutman, “Demonstration of model-independent control of the longitudinal phase space of electron beams in the linac-coherent light source with femtosecond resolution”, *Phys. Rev. Lett.*, vol. 121, no. 4, p. 044 801, 2018.
doi:10.1103/PhysRevLett.121.044801
- [4] A. Scheinker and M. Krstić, “Minimum-seeking for clfs: Universal semiglobally stabilizing feedback under unknown control directions”, *IEEE Trans. Autom. Control*, vol. 58, no. 5, pp. 1107–1122, 2012.
doi:10.1109/TAC.2012.2225514
- [5] M. Rautela, A. Williams, and A. Scheinker, “A conditional latent autoregressive recurrent model for generation and fore-

- casting of beam dynamics in particle accelerators”, *Sci. Rep.*, vol. 14, no. 1, p. 18 157, 2024.
 doi:10.1038/s41598-024-68944-0
- [6] C. Leon and A. Scheinker, “Physics-constrained machine learning for electrodynamics without gauge ambiguity based on fourier transformed maxwell’s equations”, *Sci. Rep.*, vol. 14, no. 1, p. 14 809, 2024.
 doi:10.1038/s41598-024-65650-9
- [7] C. Leon, P. M. Anisimov, N. Yampolsky, and A. Scheinker, “Utilizing neural networks to speed up coherent synchrotron radiation computations”, in *Proc. 15th International Particle Accelerator Conference*, Nashville, TN, pp. 901–904, 2024.
 doi:10.18429/JACoW-IPAC2024-MOPS73
- [8] C. Mayes, *Christophermayes/pycsr3d: PyCSR3D version 0.2.0*, version v0.2.0, 2021. doi:10.5281/zenodo.5496096
- [9] Y. Cai, “Coherent synchrotron radiation by electrons moving on circular orbits”, *Phys. Rev. Accel. Beams*, vol. 20, no. 6, p. 064 402, 2017.
 doi:10.1103/PhysRevAccelBeams.20.064402
- [10] Y. Cai and Y. Ding, “Three-dimensional effects of coherent synchrotron radiation by electrons in a bunch compressor”, *Phys. Rev. Accel. Beams*, vol. 23, no. 1, p. 014 402, 2020.
 doi:10.1103/PhysRevAccelBeams.23.014402
- [11] Y. Cai, “Two-dimensional theory of coherent synchrotron radiation with transient effects”, *Phys. Rev. Accel. Beams*, vol. 24, no. 6, p. 064 402, 2021.
 doi:10.1103/physrevaccelbeams.24.064402
- [12] O. Ronneberger, P. Fischer, and T. Brox, “U-net: Convolutional networks for biomedical image segmentation”, in *Medical Image Computing and Computer-Assisted Intervention – MICCAI 2015*, pp. 234–241, 2015.
 doi:10.1007/978-3-319-24574-4_28
- [13] A. Scheinker and R. Pokharel, “Physics-constrained 3D convolutional neural networks for electrodynamics”, *APL Mach. Learn.*, vol. 1, no. 2, p. 026 109, 2023.
 doi:10.1063/5.0132433
- [14] A. Bormanis, C. A. Leon, and A. Scheinker, “Solving the Orszag–Tang vortex magnetohydrodynamics problem with physics-constrained convolutional neural networks”, *Phys. Plasmas*, vol. 31, no. 1, p. 012 101, 2024.
 doi:10.1063/5.0172075